

Proton radii of ${}^{4,6,8}\text{He}$ isotopes from high-precision nucleon-nucleon interactions

E. Caurier*

³*Institut de Recherches Subatomiques (IN2P3-CNRS-Université Louis Pasteur)
Batiment 27/1, 67037 Strasbourg Cedex 2, France*

P. Navrátil†

Lawrence Livermore National Laboratory, P.O. Box 808, L-414, Livermore, CA 94551, USA

(Dated: February 9, 2008)

Recently, precision laser spectroscopy on ${}^6\text{He}$ atoms determined accurately the isotope shift between ${}^4\text{He}$ and ${}^6\text{He}$ and, consequently, the charge radius of ${}^6\text{He}$. A similar experiment for ${}^8\text{He}$ is under way. We have performed large-scale *ab initio* calculations for ${}^{4,6,8}\text{He}$ isotopes using high-precision nucleon-nucleon (NN) interactions within the no-core shell model (NCSM) approach. With the CD-Bonn 2000 NN potential we found point-proton root-mean-square (rms) radii of ${}^4\text{He}$ and ${}^6\text{He}$ 1.45(1) fm and 1.89(4), respectively, in agreement with experiment and predict the ${}^8\text{He}$ point proton rms radius to be 1.88(6) fm. At the same time, our calculations show that the recently developed nonlocal INOY NN potential gives binding energies closer to experiment, but underestimates the charge radii.

PACS numbers: 21.60.Cs, 21.30.Fe, 24.10.Cn, 27.20.+n

Recent advances in the theory of the atomic structure of helium [1] as well as in the techniques of isotopic shift measurement made it possible to determine accurately the charge radius of ${}^6\text{He}$ [2]. Precision laser spectroscopy on individual ${}^6\text{He}$ atoms confined and cooled in a magneto-optical trap was performed and measured the isotope shift between ${}^6\text{He}$ and ${}^4\text{He}$. With the help of precise quantum mechanical calculations with relativistic and QED corrections [3] and from the knowledge of the charge radius of ${}^4\text{He}$ (1.673(1) [4]), it was possible to determine the charge radius of ${}^6\text{He}$ to be 2.054 ± 0.014 fm [2]. The large difference between the ${}^4\text{He}$ and ${}^6\text{He}$ charge radii is due to the extra two loosely bound neutrons in ${}^6\text{He}$ that form a halo [5]. A similar experiment to determine the charge radius of ${}^8\text{He}$ is under way [6].

It is a challenge for *ab initio* many-body methods to calculate the nuclear radii with an accuracy comparable to current experimental accuracy and test in this way the nuclear Hamiltonians used as the input of *ab initio* calculations. At present, there are two *ab initio* approaches capable of describing simultaneously the ${}^4\text{He}$, ${}^6\text{He}$ and ${}^8\text{He}$ isotopes starting from realistic inter-nucleon interactions. One is the Green's function Monte Carlo (GFMC) method [7] and the other is the *ab initio* no-core shell model (NCSM) [8]. In this paper, we calculate the ground-state properties of ${}^4\text{He}$, ${}^6\text{He}$ and ${}^8\text{He}$ within the NCSM. We test two vastly different accurate nucleon-nucleon (NN) potentials, the CD-Bonn [9] and the INOY (Inside Nonlocal Outside Yukawa) [10, 11].

In the NCSM, we consider a system of A point-like non-relativistic nucleons that interact by realistic two- or two- plus three-nucleon interactions. The calculations are

performed using a finite harmonic oscillator (HO) basis. As in the present application we aim at describing loosely bound states, it is desirable to include as many terms as possible in the expansion of the total wave function. By restricting our study to two-nucleon (NN) interactions, even though the NCSM allows for the inclusion of three-body forces [12], we are able to maximize the model space and to better observe the convergence of our results. The NCSM theory was outlined in many papers. Here we only repeat the main points.

We start from the intrinsic two-body Hamiltonian for the A -nucleon system $H_A = T_{rel} + \mathcal{V}$, where T_{rel} is the relative kinetic energy and \mathcal{V} is the sum of two-body nuclear and Coulomb interactions. Since we solve the many-body problem in a finite HO basis space, it is necessary that we derive a model-space dependent effective Hamiltonian. For this purpose, we perform a unitary transformation [8, 13, 14, 15] of the Hamiltonian, which accommodates the short-range correlations. In general, the transformed Hamiltonian is an A -body operator. Our simplest, yet non-trivial, approximation that we employ in this work is to develop a two-particle cluster effective Hamiltonian, while the next improvement is to include three-particle clusters, and so on. The effective interaction is then obtained from the decoupling condition between the model space and the excluded space for the two-nucleon transformed Hamiltonian. The resulting two-body effective Hamiltonian depends on the nucleon number A , the HO frequency Ω , and N_{\max} , the maximum many-body HO excitation energy defining the model space. It follows that the effective interaction, which is translationally invariant, approaches the starting bare interaction for $N_{\max} \rightarrow \infty$. Consequently, by construction the method is convergent to the exact solution. At the same time, the NCSM effective interaction method is not variational as higher-order terms may contribute with either sign to total binding.

*etienne.caurier@ires.in2p3.fr

†navratil1@llnl.gov

Once the effective interaction is derived, we diagonalize the effective Hamiltonian in a Slater determinant (SD) HO basis that spans a complete $N_{\max}\hbar\Omega$ space. We have reached model spaces of $N_{\max} = 22, 16$ and 12 for ${}^4\text{He}$, ${}^6\text{He}$ and ${}^8\text{He}$, respectively. This is a highly non-trivial problem. The dimensions are large, e.g. 7×10^8 for ${}^6\text{He}$, although still smaller than in standard shell model calculations, e.g. the dimension is 10^9 for ${}^{56}\text{Ni}$ in full fp -shell. The first difficulty is due to the large number of shells. In the $N_{\max} = 22$ model space, there are 276 nlj -shells corresponding to 4600 $nljm$ individual states. This can be compared 4 and 20, respectively for ${}^{56}\text{Ni}$ in full fp -shell. This means that one has to handle a huge number of operators. Therefore, it has been necessary to write a specialized version of the shell model code Antoine [16, 17], suitable for the NCSM applications, see, e.g., Refs. [18, 19]. The code works in the M scheme for basis states, and uses the Lanczos algorithm for diagonalization. Its basic idea is to write the basis states as a product of two Slater determinants, a proton one and a neutron one. Matrix elements of operators are calculated for each separate subspace (one-body for the proton-neutron, two-body for the proton-proton and neutron-neutron). The performance of the code is the best when the ratio between the number of proton plus neutron SD and the dimension of the matrix is the least. It happens when the number of proton SD is equal the number of the neutron SD. To highlight the differences between the standard and the NCSM calculations, we note that for example, in ${}^{56}\text{Ni}$ there are 125970 neutron SD, while in ${}^6\text{He}$ and ${}^8\text{He}$ there are 19.5×10^6 and 43×10^6 neutron SD, respectively. Further, for example, in the basis of ${}^{48}\text{Ca}$ the 12022 neutron SD with $M = 0$ produce 144528484 states in the full basis. In ${}^8\text{He}$, the 8986408 neutron SD with $M = 0$ produce only 56216057 states in the full basis and 7007190 of these SD that have $N = 12$ are associated with a unique $N = 0$ proton SD. Another comment concerning the difficulty of performing the NCSM calculations is that the matrices become less sparse when the number of particles decrease. To keep the comparison with the standard shell model, in ${}^4\text{He}$ we have a dimension 12.5 smaller than in ${}^{56}\text{Ni}$ but 1.5 times more non-zero matrix elements. For all these reasons, NCSM calculations with large N_{\max} model spaces are difficult but still feasible with a computer with a large RAM memory and a large disk capacity. As a last example, one Lanczos iteration in ${}^6\text{He}$ takes 7 hours while the same in ${}^{56}\text{Ni}$ takes 70 minutes on an Opteron machine.

As already mentioned, we test two different, high-precision NN interactions in this study: the CD-Bonn 2000 [9] and the INOY [10, 11] potentials.

The CD-Bonn 2000 potential [9] as well as its earlier version [20] is a charge-dependent NN interaction based on one-boson exchange. It is described in terms of covariant Feynman amplitudes, which are non-local. Consequently, the off-shell behavior of the CD-Bonn interaction differs from local potentials which leads to larger binding energies in nuclear few-body systems.

TABLE I: Point-proton (r_p) and point-neutron (r_n) rms radii and binding energies (E_B) of ${}^{4,6,8}\text{He}$ isotopes. The calculated values were obtained within the *ab initio* NCSM. The experimental values are from Refs. [2, 4, 5, 22, 23, 24, 25].

r_p [fm]	Expt.	CD-Bonn 2000	INOY
${}^4\text{He}$	1.455(1)	1.45(1)	1.37(1)
${}^6\text{He}$	1.912(18)	1.89(4)	1.76(3)
${}^8\text{He}$		1.88(6)	1.74(6)
r_n [fm]	Expt.	CD-Bonn 2000	INOY
${}^6\text{He}$	2.59-2.85	2.67(5)	2.55(10)
${}^8\text{He}$	2.69(4)	2.80(10)	2.60(10)
E_B [MeV]	Expt.	CD-Bonn 2000	INOY
${}^4\text{He}$	28.296	26.16(6)	29.10(5)
${}^6\text{He}$	29.269	26.9(3)	29.38(10)
${}^8\text{He}$	31.408(7)	26.0(4)	30.30(30)

A new type of interaction, which respects the local behavior of traditional NN interactions at longer ranges but exhibits a non-locality at shorter distances, was recently proposed by Doleschall *et al.* [10, 11]. The authors explore the extent to which effects of multi-nucleon forces can be absorbed by non-local terms in the NN interaction. They investigated if it is possible to introduce non-locality in the NN interaction so that it correctly describes the three-nucleon bound states, while still reproducing NN scattering data with high precision. The so called IS version of this interaction, introduced in Ref. [10], contains short-range non-local potentials in 1S_0 and 3S_1 - 3D_1 partial waves while higher partial waves are taken from Argonne v_{18} . In this study we are using the IS-M version, which includes non-local potentials also in the P and D waves [11]. We note that, for this particular version, the on-shell properties of the triplet P -wave interactions have been modified in order to improve the description of $3N$ analyzing powers. Unfortunately, this gives a slightly worse fit to the Nijmegen 3P phase shifts.

We performed ${}^4\text{He}$ calculations both in the Slater determinant basis using the Antoine code and model spaces up to $N_{\max} = 22$ within the two-body effective interaction approximation and the Jacobi-coordinate HO basis using the Manyeff code [13] with model spaces up to $N_{\max} = 20$ within either the two-body effective interaction approximation or the three-body effective interaction approximation. The ground-state energy convergence is good for both NN potentials. For the CD-Bonn 2000, this can be seen in Fig. 1 of Ref. [21]. Our ${}^4\text{He}$ binding energy and point-proton root-mean-square (rms) radii results are summarized in Table I. We note that the point-proton rms radius is related to the proton charge rms radius as [2] $\langle r_p^2 \rangle = \langle r_c^2 \rangle - \langle R_p^2 \rangle - \langle R_n^2 \rangle (N/Z)$, with $(\langle R_p^2 \rangle)^{1/2} = 0.895(18)$ fm [26], the charge radius of the proton and $\langle R_n^2 \rangle = -0.120(5)$ fm² [27], the mean-square-charge radius of the neutron. We observe that the CD-Bonn 2000 underbinds ${}^4\text{He}$ by about 2 MeV, but describes the point-proton rms radius in agreement with experiment. The INOY NN potential, on the other

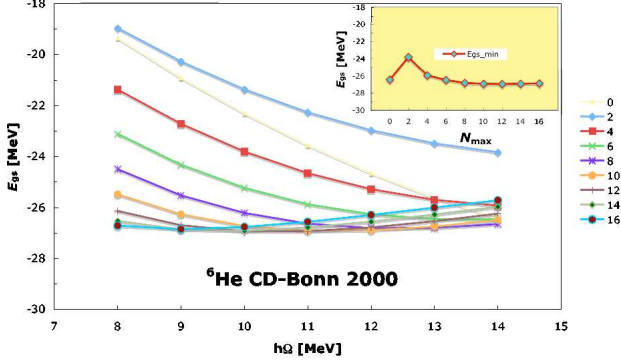


FIG. 1: The ${}^6\text{He}$ ground-state energy dependence on the HO frequency for different model-spaces sizes from $N_{\text{max}} = 0$ to $N_{\text{max}} = 16$ obtained using the CD-Bonn 2000 NN potential. The inset demonstrates how the values at the minima of each curve converge with increasing N_{max} .

hand, overbinds ${}^4\text{He}$ by 800 keV and underestimates the point-proton rms radius. We note that our INOY ${}^4\text{He}$ results are in perfect agreement with those obtained by the Faddeev-Yakubovski calculations of Ref. [28].

Our calculations for ${}^6\text{He}$ and ${}^8\text{He}$ nuclei were performed in model spaces up to $N_{\text{max}} = 16$ and $N_{\text{max}} = 12$, respectively, for a wide range of HO frequencies.

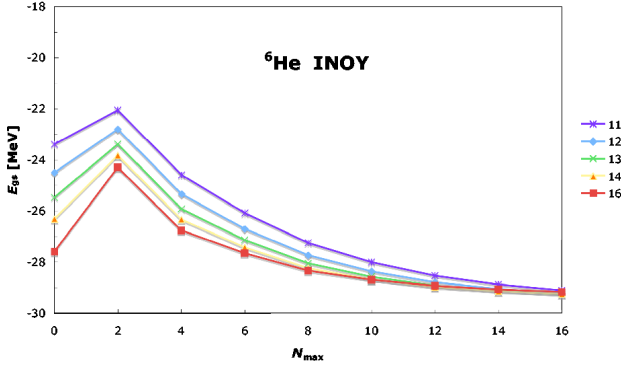


FIG. 2: The ${}^6\text{He}$ ground-state energy dependence on the model space size for different HO frequencies from $\hbar\Omega = 11$ MeV to $\hbar\Omega = 16$ MeV obtained using the INOY NN potential.

The ${}^6\text{He}$ ground-state energy dependence on the HO frequency for different model spaces is shown in Fig. 1 for the CD-Bonn 2000. In Fig. 2, we show the ${}^6\text{He}$ ground-state energy dependence on the model-space size for different HO frequencies obtained using the INOY NN potential. We observe a quite different convergence trend for the two potentials. For the INOY, the convergence is very uniform with respect to the HO frequency with systematic changes with N_{max} . The convergence with increasing N_{max} is evident. We extrapolate, e.g. assuming an exponential dependence on N_{max} as $E(N_{\text{max}}) = E_{\infty} + a \exp(-bN_{\text{max}})$, that the converged INOY ground-state energy will slightly overbind ${}^6\text{He}$. The ground-state energy convergence for the CD-Bonn

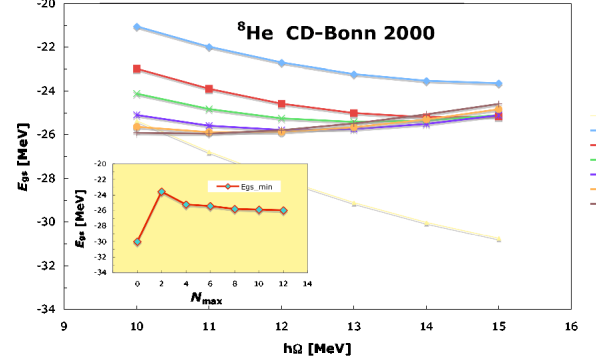


FIG. 3: The same as in Fig. 1, but for ${}^8\text{He}$ and model-spaces from $N_{\text{max}} = 0$ to $N_{\text{max}} = 12$.

2000 is quite different with a stronger dependence on the frequency, with minima shifting to lower frequency with basis size increase, and an overall weaker dependence on N_{max} as seen in the inset of Fig. 1. Contrary to the INOY, the CD-Bonn underbinds ${}^6\text{He}$ by more than 2 MeV, which is typical for the standard high-precision NN potentials [7].

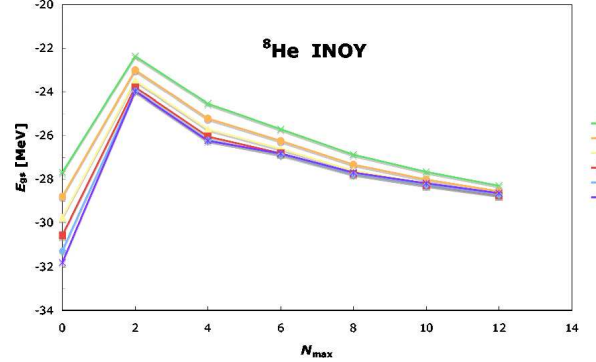


FIG. 4: The same as in Fig. 2, but for ${}^8\text{He}$ and HO frequencies from $\hbar\Omega = 12$ MeV to $\hbar\Omega = 17$ MeV.

The same ground-state energy dependencies for ${}^8\text{He}$ are shown in Figs. 3 and 4. Here, the INOY extrapolation is more difficult as, due to the complexity of the calculations, we are limited to model spaces up to $N_{\text{max}} = 12$. Our binding energy results are summarized in Table I. The CD-Bonn 2000 and the INOY NN potentials underbind ${}^8\text{He}$ by about 5 MeV and 1 MeV, respectively. Our calculation suggest that the CD-Bonn 2000 predicts ${}^6\text{He}$ bound but ${}^8\text{He}$ unbound. The INOY predicts both ${}^6\text{He}$ and ${}^8\text{He}$ bound. The isospin dependence of the binding energies is wrong for the CD-Bonn. A very similar situation was found for the Argonne NN potentials in Ref. [7]. Those NN potentials, at the same time, predict also the ${}^6\text{He}$ unbound [7]. The CD-Bonn NN potential must be augmented by three-nucleon interaction to achieve a correct description of binding energies. The INOY NN potential improves on the isospin dependence of binding energies. As this potential absorbs some three-

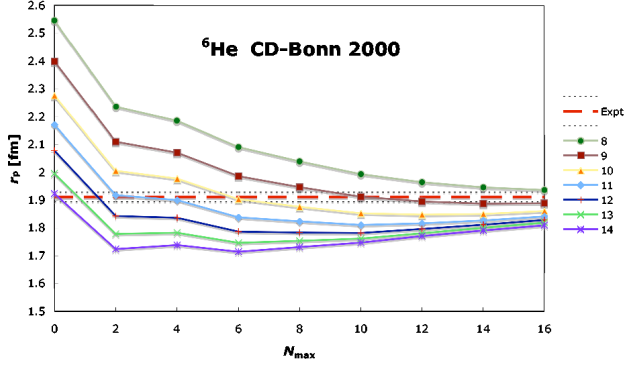


FIG. 5: The ${}^6\text{He}$ point-proton rms radius dependence on the model space size for different HO frequencies from $\hbar\Omega = 8$ MeV to $\hbar\Omega = 14$ MeV obtained using the CD-Bonn 2000 NN potential. The experimental value is from Ref. [2].

nucleon effects in its nonlocal part, it supports the expectation that a three-nucleon interaction should improve the isospin dependence of binding energies. At the same time, a three-nucleon interaction can hardly be added to the INOY NN potential as it was already fine-tuned to reproduce $A = 3$ binding energies. Therefore, it is difficult to see, how to correct its still not quite right binding energy predictions for the He isotopes.

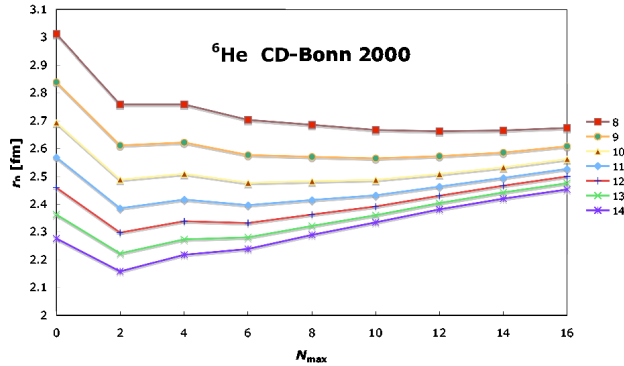


FIG. 6: The ${}^6\text{He}$ point-neutron rms radius dependence on the model space size for different HO frequencies from $\hbar\Omega = 8$ MeV to $\hbar\Omega = 14$ MeV obtained using the CD-Bonn 2000 NN potential.

Our point-nucleon rms results are presented in Figs. 5-9 and summarized in Table I. In the figures, we show the model-space size dependence of the rms radii for different HO frequencies. A general feature is a decrease of the HO frequency dependence with increasing model-space size defined by N_{max} . In all cases, the rms radii exhibit convergence. The ${}^6\text{He}$ point-proton rms radius experimental value is shown as a dashed line in Figs. 5 and 7 with the dotted lines indicating the experimental error. The CD-Bonn 2000 ${}^6\text{He}$ point-proton rms radius, Fig. 5, stabilizes at $N_{\text{max}} = 16$ for the HO frequencies of $\hbar\Omega = 9$ and 10 MeV, while it is still decreasing for $\hbar\Omega = 8$ MeV and it is increasing for the HO frequencies higher than $\hbar\Omega = 10$

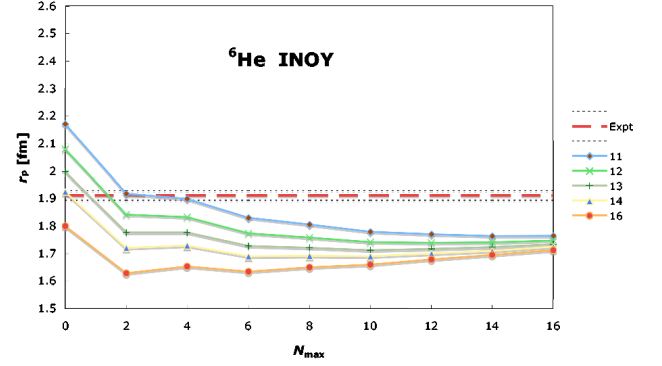


FIG. 7: The same as in Fig. 5, but for the INOY NN potential and HO frequencies from $\hbar\Omega = 11$ MeV to $\hbar\Omega = 16$ MeV.

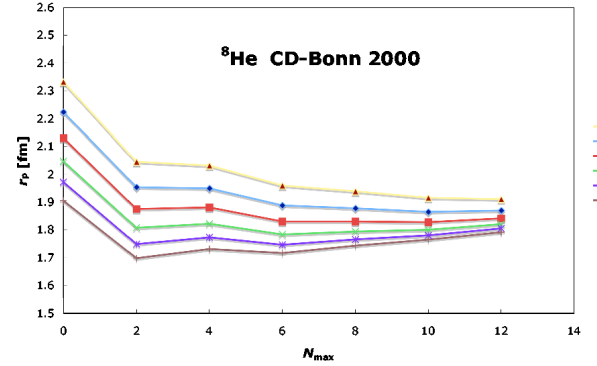


FIG. 8: The ${}^8\text{He}$ point-proton rms radius dependence on the model space size for different HO frequencies from $\hbar\Omega = 10$ MeV to $\hbar\Omega = 15$ MeV obtained using the CD-Bonn 2000 NN potential.

MeV. Clearly, the stable result is very close to the experimental value. We estimate the error of our calculation at $N_{\text{max}} = 16$ from the HO frequency dependence. We note that we published the ${}^6\text{He}$ CD-Bonn point-proton rms radii in Ref. [29]. Those results were obtained using the HO frequency of $\hbar\Omega = 13$ MeV in $N_{\text{max}} = 6, 8$ and 10 model spaces. Our $N_{\text{max}} = 10$ value, 1.763 fm, was then compared to experiment in Ref. [2]. We can see from Fig. 5 that the radius is still increasing with N_{max} for that frequency and reaches, e.g. 1.819 fm at $N_{\text{max}} = 16$. From our present results obtained up to $N_{\text{max}} = 16$ for a wide range of HO frequencies we arrive at the CD-Bonn 2000 point-proton rms radius of 1.89(4) fm that, taken into account the error bars, agrees with the experimental value of 1.912(18) fm. The point-neutron rms radius shows a stronger dependence on the HO frequency and a slower convergence as seen in Fig. 6. This is to be expected as the neutron halo is extended and a large HO basis is needed to describe it properly. Nevertheless, we observe a reasonable stability of the neutron rms radius at lower HO frequencies that allows us to estimate its CD-Bonn 2000 value to be 2.67(5) fm.

We observe a better convergence for the INOY NN potential not only for the binding energies but also for

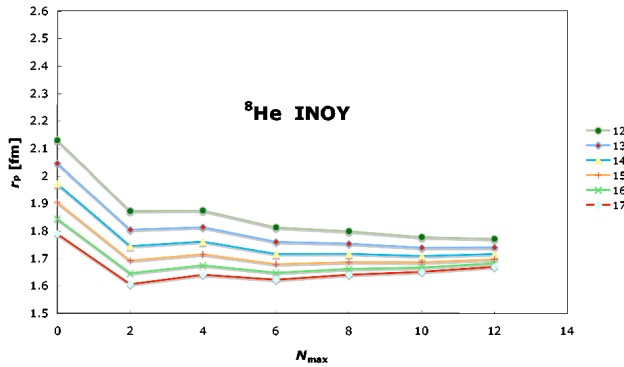


FIG. 9: The same as in Fig. 8, but for the INOY NN potential and HO frequencies from $\hbar\Omega = 12$ MeV to $\hbar\Omega = 17$ MeV.

the radii. This is apparent from Fig. 7. For this NN potential, we find the ${}^6\text{He}$ point-proton rms radius to be 1.76(3) fm. This is significantly less than in experiment. Clearly, the INOY NN potential underpredicts both the ${}^4\text{He}$ and ${}^6\text{He}$ point-proton rms radii.

Our ${}^8\text{He}$ point-proton rms radius results are shown in Figs. 8 and 9 for the CD-Bonn 2000 and INOY potentials, respectively. Based on the basis size and the HO frequency dependence, we predict the ${}^8\text{He}$ point-proton rms radius to be 1.88(6) fm based on our CD-Bonn results. The INOY NN potential gives a smaller value, 1.74(6) fm, consistently with the smaller ${}^4\text{He}$ and ${}^6\text{He}$ results. In both cases, the ${}^8\text{He}$ point-proton radius is

slightly smaller than the corresponding one in ${}^6\text{He}$. Taking into account the uncertainties, however, the differences are insignificant.

In conclusion, we performed large-scale *ab initio* NCSM calculations for ${}^4\text{He}$, ${}^6\text{He}$ and ${}^8\text{He}$ isotopes. We used the high-precision CD-Bonn 2000 and the INOY NN potentials and obtained results for binding energies and point-nucleon rms radii. Using the CD-Bonn 2000, we obtained the point-proton rms radii of ${}^4\text{He}$ and ${}^6\text{He}$ in agreement with experiment and predict the ${}^8\text{He}$ point-proton rms radius to be 1.88(6) fm. The INOY NN potential, on the other hand, underestimates both ${}^4\text{He}$ and ${}^6\text{He}$ experimental point-proton rms radii. The CD-Bonn 2000 underbinds the He isotopes as is typical for the standard high-precision NN interactions. It must be augmented by a three-nucleon interaction. It is conceivable that this can be done in a way that will not change the charge radii. The INOY NN potential gives binding energies closer to experiment. However, it is not obvious, how the charge radii results can be brought to agreement with experiment when using this potential. It can hardly be augmented by a three-nucleon interaction as it was already fine-tuned to describe the $A = 3$ system.

This work was partly performed under the auspices of the U. S. Department of Energy by the University of California, Lawrence Livermore National Laboratory under contract No. W-7405-Eng-48. Support from the LDRD contract No. 04-ERD-058, and from U.S. DOE, OS (Work Proposal Number SCW0498) is acknowledged.

-
- [1] G. W. F. Drake, in *Long-Range Casimir Forces: Theory and Recent Experiments in Atomic Systems* edited by F. S. Levin and D. Micha (Plenum Press, New York, 1993), pp. 107-217.
 - [2] L.-B. Wang *et al.*, Phys. Rev. Lett. **93**, 142501 (2004).
 - [3] G. W. F. Drake, Nucl Phys. **A737**, 25 (2004).
 - [4] E. Borie and G. A. Rinker, Phys. Rev. A **18**, 324 (1978).
 - [5] I. Tanihata, D. Hirata, T. Kobayashi, S. Shimoura, K. Sugimoto and H. Toki, Phys. Lett. B **289**, 261 (1992).
 - [6] P. Mueller *et al.*, Bul. Am. Phys. Soc. **50**, No. 6, p. 56 (2005).
 - [7] S. C. Pieper, R. B. Wiringa, and J. Carlson, Phys. Rev. C **70**, 054325 (2004).
 - [8] P. Navrátil, J. P. Vary and B. R. Barrett, Phys. Rev. Lett. **84**, 5728 (2000); Phys. Rev. C **62**, 054311 (2000).
 - [9] R. Machleidt, Phys. Rev. C **63**, 024001 (2001).
 - [10] P. Doleschall, I. Borbély, Z. Papp, and W. Plessas, Phys. Rev. C **67**, 0064005 (2003).
 - [11] P. Doleschall, Phys. Rev. C **69**, 054001 (2004).
 - [12] P. Navrátil and W. E. Ormand, Phys. Rev. C **68**, 034305 (2003).
 - [13] P. Navrátil, G. P. Kamuntavičius and B. R. Barrett, Phys. Rev. C **61**, 044001 (2000).
 - [14] K. Suzuki and S. Y. Lee, Prog. Theor. Phys. **64**, 2091 (1980).
 - [15] K. Suzuki and R. Okamoto, Prog. Theor. Phys. **92**, 1045 (1994).
 - [16] E. Caurier, G. Martinez-Pinedo, F. Nowacki, A. Poves, J. Retamosa and A. P. Zuker, Phys. Rev. C **59**, 2033 (1999).
 - [17] E. Caurier and F. Nowacki, Acta Physica Polonica B **30**, 705 (1999).
 - [18] E. Caurier, P. Navrátil, W. E. Ormand and J. P. Vary, Phys. Rev. C **64**, 051301 (2001).
 - [19] E. Caurier, P. Navrátil, W. E. Ormand and J. P. Vary, Phys. Rev. C **66**, 024314 (2002).
 - [20] R. Machleidt, F. Sammarruca and Y. Song, Phys. Rev. C **53**, 1483 (1996).
 - [21] P. Navrátil, W. E. Ormand, C. Forssén and E. Caurier, Eur. Phys. J. A **25**, s01, 481 (2005).
 - [22] G. D. Alkhalazov *et al.*, Phys. Rev. Lett. **78**, 2313 (1997).
 - [23] V. B. Shostak, G. P. Palkin, N. I. Woloshin, V. P. Likhachev, M. N. Martins and M. T. F. da Cruz, Phys. Rev. C **63**, 017602 (2000).
 - [24] D. R. Tilley *et al.*, Nucl. Phys. A **708**, 3 (2002).
 - [25] J. H. Kelley *et al.*, Nucl. Phys. A **745**, 155 (2004).
 - [26] I. Sick, Phys. Lett. B **576**, 62 (2003).
 - [27] S. Kopecky *et al.*, Phys. Rev. Lett. **74**, 2427 (1995); S. Kopecky *et al.*, Phys. Rev. C **56**, 2229 (1997).
 - [28] R. Lazauskas and J. Carbonell, Phys. Rev. C **70**, 044002 (2004).
 - [29] P. Navrátil, J. P. Vary, W. E. Ormand and B. R. Barrett, Phys. Rev. Lett. **87**, 172502 (2001).